Hindawi Publishing Corporation
Mathematical Problems in Engineering
Volume 2015, Article ID 619430, 8 pages
http://dx.doi.org/10.1155/2015/619430

Research Article

Model Free Command Filtered Backstepping Control for Marine Power Systems

Hongcheng Zhou,[1,2] Dezhi Xu,[3] and Bin Jiang[1]

[1]*College of Automation Engineering, Nanjing University of Aeronautics and Astronautics, No. 29, Yudao Road, Nanjing 210016, China*
[2]*Institute of Information, JinLing Institute of Technology, No. 99, Hongjing Road, Nanjing 211169, China*
[3]*Key Laboratory of Advanced Process Control for Light Industry (Ministry of Education), Institute of Automation, Jiangnan University, No. 1800, Lihu Road, Wuxi 214122, China*

Correspondence should be addressed to Dezhi Xu; lutxdz@126.com

Received 17 April 2015; Accepted 16 July 2015

Academic Editor: Xinggang Yan

In order to retrain chaotic oscillation of marine power systems which are excited by periodic electromagnetism perturbation, two novel model free command-filtered backstepping control methods are designed in this paper. Firstly, the dynamic model of marine power system based on the two parallel nonlinear models is established. Secondly, extended state observer (ESO) and adaptive neural network observer (NNO) are designed to estimate the velocity signal and the unknown dynamic model. Moreover, the uniform form of ESO and NNO is given. Next, the model free command-filtered backstepping controller is put forward based on the uniform observer form. Finally, the simulation results indicate that the two proposed control algorithms can quickly retrain chaotic oscillation and their effectiveness and potential are amply demonstrated.

1. Introduction

The structure of modern marine power systems has been evermore complicated, especially the emergence of high-performance ship electric propulsion applications. With the development of modern marine power system, more reliable and stable requirements are needed for marine power systems. In recent years, researchers have found that chaotic oscillations occur in marine power system during the voyage or paroxysmal bursts. Chaotic oscillations could lead to the system instability, which poses a potential threat to the safe operation of the marine power grid [1–3].

At present, most of the power system chaos control methods mainly focus on land-based power systems, such as adaptive control, feedback control, and inverse system control [2, 4–7]. Obviously, the marine power systems can be regarded as a special case of land-based power systems. As a result, a large number of control methods of land-based power systems can be extended to marine power systems. However, in the actual system, the accurate value of speed signal and the model parameters are difficult to obtain, which will make many model-based control algorithms difficult to be applied [8].

In control theory, backstepping is a technique developed in the 1990s for designing stabilizing controls for a special class of nonlinear dynamical systems [9], which has wider application range than output feedback [10, 11]. These systems are built from subsystems that radiate out from an irreducible subsystem stabilized by using some other methods. Thanks to this recursive structure, the designer can start the design process at the known-stable system and "back out" new controllers that progressively stabilize each outer subsystem. The process terminates when the final external control is reached. Therefore, this process is known as backstepping. So far, backstepping control has made a lot of achievements, such as adaptive backstepping control, adaptive sliding mode backstepping control, and dynamic surface control [12–14].

Recently, model free control has increasingly received more attention in solving complex and practical problems, such as active disturbance rejection control (ADRC) [15], model free adaptive control (MFAC) [16–18], and intelligent control [19]. Based on the aforementioned works, this paper

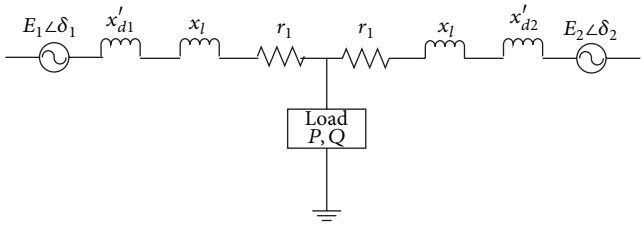

Figure 1: Block diagram of marine power systems.

develops two model free adaptive backstepping controls with command-filtered compensation for marine power systems. In order to suppress the chaotic marine power system oscillations, based on extended state observer (ESO) and adaptive neural network observer (NNO), the model free adaptive command-filtered backstepping chaos controller is designed. The rest of this paper is organized as follows. In Section 2, a brief description of two parallel nonlinear mathematical models is introduced. In Section 3, ESO and adaptive NNO are designed to estimate the velocity signal and the unknown dynamic model. Moreover, the uniform form of ESO and NNO is given. In Section 4, the model free command-filtered backstepping controller is proposed based on the uniform observer form. Simulation results are presented to show the effectiveness of the proposed control technique in Section 5. Finally, some conclusions are made in Section 6.

2. Marine Power System Modeling and Problem Formulation

The basic structure of the power supply network for marine power system can be expressed as Figure 1, where $E_1\angle\delta_1$ and $E_2\angle\delta_2$ are emf of two generators in the system, respectively. x'_{d1} and x'_{d2} are synchronous reactances of two generators, respectively. x_l and r_l are the line resistance and reactance, respectively. P and Q denote the system loads. Because of the short-circuit in the marine power system, the line resistance is very small, which can often be neglected.

Considering the same case of generator parameters, let $\delta = \delta_1 - \delta_2$ and $\omega = \omega_1 - \omega_2$ become the relative power angle and relative power angle velocity of the two equivalent generators. Then two machines interconnected system can be described as follows:

$$\begin{aligned} \frac{d\delta}{dt} &= \omega, \\ H\frac{d\omega}{dt} &= P_m - D\omega - P_e\left(1 + \Delta p\cos\left(\beta t\right)\right)\sin\delta, \end{aligned} \tag{1}$$

where H and D are equivalent inertia and damping, respectively. P_m is the input mechanical power of generator; P_e denotes the electromagnetic power of system output. $P_e \cdot \Delta p\cos\beta t$ represents the electromagnetic perturbation introduced to study chaotic motion for the marine power system under disturbance. $P_e \cdot \Delta p$ expresses the amplitude of disturbance, and β describes the frequency of disturbance.

Through the transformation $\tau = t\sqrt{P_e/H}$, $x_1(\tau) = \delta(t)$, and $x_2(\tau) = \sqrt{H/P_e}\omega(t)$. Equation (1) can be written as

$$\begin{aligned} \frac{dx_1}{d\tau} &= x_2, \\ \frac{dx_2}{d\tau} &= -\sin x_1 - \lambda x_2 + \rho + \mu\cos\left(\gamma\tau\right)\sin x_1, \end{aligned} \tag{2}$$

where $\lambda = D\sqrt{P_e/H}$, $\rho = P_m/P_e$, $\mu = \Delta p$, and $\gamma = \beta\sqrt{P_e/H}$. According to the transformation, we know that the system state variables x_1 and x_2 are obtained by the transformation of δ and ω, which have the physical meanings of the power angle error and the power angle error relative velocity between the two generators. However, if the value $\sqrt{H/P_e}$ is imprecise, accurate state $x_2(\tau)$ cannot be gained. In the following works, a novel model free control method is proposed under one condition; that is, only power angle $\delta(t)$ can be measured.

In order to ascertain subject for further elaboration, we define $\dot{a} = da/d\tau$. In this paper, then (2) can be rewritten as

$$\begin{aligned} \dot{x}_1 &= x_2, \\ \dot{x}_2 &= -\sin x_1 - \lambda x_2 + \rho + \mu\cos\left(\gamma\tau\right)\sin x_1. \end{aligned} \tag{3}$$

Let $x = [x_1, x_2]^T$, and $f(x) = -\sin x_1 - \lambda x_2 + \rho + \mu\cos(\gamma\tau)\sin x_1$. In the above marine power system (3), when amplitude μ and frequency γ of disturbance satisfy certain conditions, the chaotic motion will occur. In the case of suppressing the chaotic motion, a controlled input u must be added to the equation of state (3); namely,

$$\begin{aligned} \dot{x}_1 &= x_2, \\ \dot{x}_2 &= f\left(x\right) + u, \\ y &= x_1. \end{aligned} \tag{4}$$

If the parameters of model (3) cannot be obtained, $f(x)$ can be regarded as an unknown function, and the state x_2 also cannot be measured.

3. Observer-Based Model Identification and State Estimation

In this section, there are two methods proposed to estimate the $f(x)$ and the state x_2 of (4). One is the ESO method; the other is the neural network observer method.

3.1. Extended State Observer Design. It is assumed that only power angle $\delta = y$ can be measured for marine power system (3). Hence in this paper, the third-order ESO is designed, which is used to estimate the state x_2 and the unknown function $f(x)$. Define the unknown function $f(x)$ as an extended state x_3. Let $x_3 = f(x)$ and $\dot{x}_3 = \bar{\omega}$, where $\bar{\omega}(t)$

is an unknown function. Assume that $|\varpi(t)| < r$, and then system (4) is equivalent to

$$\begin{aligned} \dot{x}_1 &= x_2, \\ \dot{x}_2 &= x_3 + u, \\ \dot{x}_3 &= \varpi, \\ y &= x_1. \end{aligned} \tag{5}$$

For purpose of estimating the state x_2 and the unknown function $f(x)$, the following third-order ESO [13, 17] is designed:

$$\begin{aligned} \dot{\hat{x}}_1 &= \hat{x}_2 - l_1 e, \\ \dot{\hat{x}}_2 &= \hat{x}_3 + u - l_2 \mathrm{fal}\left(e, \alpha_1, \sigma_1\right), \\ \dot{\hat{x}}_3 &= -l_3 \mathrm{fal}\left(e, \alpha_2, \sigma_2\right), \\ \hat{y} &= \hat{x}_1, \end{aligned} \tag{6}$$

where $e = y - \hat{y} = x_1 - \hat{x}_1$ and $\hat{x}_1, \hat{x}_2, \hat{x}_3$ is the observer of x_1, x_2, x_3. $0 < \alpha_1 < 1, 0 < \alpha_2 < 1, \sigma_1 > 0, \sigma_2 > 0$, and $l_i > 0$, $i = 1, 2, 3$, are parameters of observer (6). And the nonlinear function fal$(\cdot)$ is defined as

$$\mathrm{fal}\left(\epsilon, \alpha, \sigma\right) = \begin{cases} |\epsilon|^{\alpha} \operatorname{sgn}\left(\epsilon\right), & |\epsilon| > \sigma, \\ \dfrac{\epsilon}{\sigma^{1-\alpha}}, & |\epsilon| \le \sigma. \end{cases} \tag{7}$$

Let T be the sampling period of control. In general, σ is selected as $\sigma = 5 \sim 10T$. Until now, there is no reliable and theoretical analysis method available for the third-order ESO. Fortunately, based on [20], if the suitable parameters of observer (6) are selected, the following results can be gained:

$$\begin{aligned} \lim_{t \to \infty} \left|\tilde{x}_2\right| &< l_1 \left(\frac{r}{l_3}\right)^{1/\alpha_2} = \varepsilon_{x_2}, \\ \lim_{t \to \infty} \left|\tilde{x}_3\right| &< l_2 \left(\frac{r}{l_3}\right)^{1/\alpha_2} = \varepsilon_{f(x)}, \end{aligned} \tag{8}$$

where $\tilde{x}_2 = x_2 - \hat{x}_2$ and $\tilde{x}_3 = x_3 - \hat{x}_3$. Hence, the suitable observer parameters can make the state estimation errors $\tilde{x}_1$ and $\tilde{x}_2$ and the function estimation error $\tilde{f}(x) = \tilde{x}_3 = \hat{f}(x) - f(x)$ uniformly ultimately bounded.

3.2. Adaptive Neural Network Observer Design. The model (4) can be represented as

$$\begin{aligned} \dot{x} &= Ax + b\left[f\left(x\right) + u\right], \\ y &= c^T x, \end{aligned} \tag{9}$$

where

$$A = \begin{bmatrix} 0 & 1 \\ 0 & 0 \end{bmatrix}, \quad b = \begin{bmatrix} 0 \\ 1 \end{bmatrix}, \quad c = \begin{bmatrix} 1 \\ 0 \end{bmatrix}. \tag{10}$$

Radical basis function (RBF) neural network is usually used to model nonlinear functions for its good capabilities in function approximation [21]. It is a well-known result that for $\overline{x}$ restricted to a compact set of S and for some sufficiently large numbers of hidden layer neurons, there exist weights and thresholds so that any continuous function on the compact set S can be represented by a recurrent neural network. The functions $f(x)$ are approximated as follows by using neural network system with $\hat{x}$, their input being estimated:

$$\hat{f}\left(\hat{x}\right) = \widehat{W}^T \Phi\left(\hat{x}\right), \tag{11}$$

where $\hat{x}$ is the estimation of x. $\widehat{W} \in R^{m \times 3}$ is the estimation weight matrix of the RBF neural network. Therein, m is the number of nodes of the implicit layer. And $\Phi(\cdot) = [\phi(\cdot), \ldots, \phi_m(\cdot)]^T$ acts as an activation function vector, which is usually assumed to be a Gaussian function as follows:

$$\phi_j\left(\overline{x}\right) = \exp\left(-\frac{\left\|\overline{x} - \nu_j\right\|^2}{\varrho_j^2}\right), \quad j = 1, \ldots, m, \tag{12}$$

where $\nu_j \in R^{3 \times 1}$ and ϱ_j represent the center vector and the width vector of the basis function, respectively. The approximating property of the nonlinear models depends on the center vector, width vector of Gaussian function, and the number of implicit layers m. The original functions $f(x)$ in (11) can be expressed as

$$f\left(x\right) = W^{*T} \Phi\left(x\right) + \varepsilon, \tag{13}$$

where ε is the functional reconstruction error of the neural network. In general, even given the best-possible weight values, the given nonlinear function is not exactly approximated and the functional reconstruction error is still remaining. W^* is the optimal parameter vector required for analytical purpose satisfying

$$W^* = \arg\min_{W} \left[\sup\left|\hat{f}\left(\hat{x}\right) - f\left(x\right)\right|\right] \tag{14}$$

with bounded as $\|W^*\| \le M$.

With the neural network approximation, the dynamic equation of a NNO which estimates the states in (4) is given as follows:

$$\begin{aligned} \dot{\hat{x}} &= A\hat{x} + b_0\left[\hat{f}\left(\hat{x}\right) + u\right] + K\left(y - c^T \hat{x}\right) \\ \hat{y} &= c^T \hat{x}, \end{aligned} \tag{15}$$

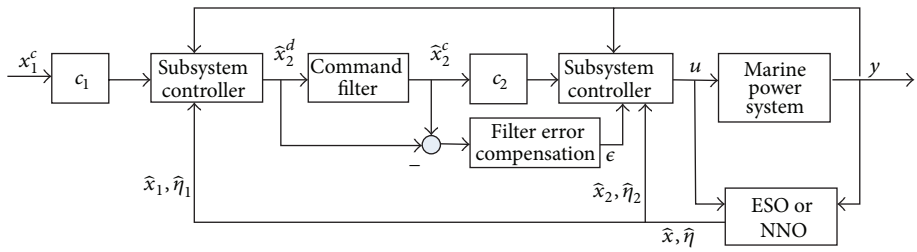

Figure 2: Proposed two model free adaptive command-filtered backstepping controls block diagram.

where $K = [k_1, k_2]^T$ is the observer gain vector; $\hat{x} = [\hat{x}_1, \hat{x}_2]^T$, and b_0 will be designed later. Define the state and the output estimated errors as $\tilde{x} = x - \hat{x}$ and yield the error dynamics from (4) and (15):

$$\begin{aligned}\dot{\tilde{x}} &= \overline{A}\tilde{x} + b_0\left[\widetilde{W}^T\Phi(\hat{x}) + u\right] \\ &\quad + (b - b_0)\left[W^{*T}\Phi(x) + u\right] + b_0 d + b\varepsilon,\end{aligned} \tag{16}$$

where $\overline{A} = A - Kc^T$, $\widetilde{W} = W^* - \widehat{W}$, and $d = W^{*T}[\Phi(x) - \Phi(\hat{x})]$. In general, the neural network basis function is bounded. This implies that every element of $\Phi(x) - \Phi(\hat{x})$ is bounded; that is, $\|\Phi(x) - \Phi(\hat{x})\| \le \Phi^M$ with Φ^M constant.

In order to construct the vector b_0, the algebraic Ricatilike equation $\overline{A}^T\Gamma + \Gamma\overline{A} + \Gamma^2 \le -Q_1$ for $Q_1 > 0$ is considered [22]. Using the positive definite matrix Γ, the vector b_0 is chosen as $b_0 = \Gamma^{-1}c$. It is shown below that this choice will guarantee the stability of the observer.

Theorem 1. *Considering the observer system (15), the update law for the parameters of the neural network system is*

$$\dot{\widehat{W}} = \bar{\gamma}\Upsilon\Phi(\hat{x}) - \kappa\Upsilon\widehat{W}, \tag{17}$$

where $\Upsilon = \Upsilon^T > 0$ *and* $\kappa > 0$. *Then, the state estimation errors* $\tilde{x}_1$, $\tilde{x}_2$ *and parameter estimation errors are uniformly ultimately bounded.*

Proof. The proof is similar as [22].

Let $b_0 = [b_{01}, b_{02}]^T$; (15) can be rewritten as

$$\begin{aligned}\dot{\hat{x}}_1 &= \hat{x}_2 + b_{01} + k_1\left(y - c^T\hat{x}\right), \\ \dot{\hat{x}}_2 &= b_{02}f(\hat{x}) + b_{02}u + k_2\left(y - c^T\hat{x}\right).\end{aligned} \tag{18}$$

Equation (19) denotes the uniform form of observers (6) and (18):

$$\begin{aligned}\dot{\hat{x}}_1 &= \hat{x}_2 + \eta_1, \\ \dot{\hat{x}}_2 &= bu + \eta_2.\end{aligned} \tag{19}$$

For ESO (6), $\eta_1 = -l_1 e$, $\eta_2 = \hat{f}(x) - l_2\mathrm{fal}(e, \alpha_1, \sigma)$, and $b = 1$. For NNO (18), $\eta_1 = b_{01} + k_1(y - c^T\hat{x})$, $\eta_2 = b_{02}\hat{f}(\hat{x}) + k_2(y - c^T\hat{x})$, and $b = b_{02}$. □

4. Command-Filtered Backstepping Controller Design

It can be seen above that (19) is a strict-feedback form, so the controller can be designed via the backstepping idea. The differential expansion and control saturation problems exist in the traditional backstepping control. Therefore, Farrell et al. have introduced a constrained command filter into the adaptive backstepping control system [23], and the command filter is used to eliminate the impact of derivative of the "virtual controls" and the control saturation. Command-filtered backstepping control is different from backstepping control, such as the design procedure. The block diagram of the proposed control algorithm is described as Figure 2.

Define the tracking error variables e_1 and e_2 which are introduced as follows:

$$\begin{aligned}e_1 &= \hat{x}_1 - x_1^c, \\ e_2 &= \hat{x}_2 - \hat{x}_2^c,\end{aligned} \tag{20}$$

where x_1^c and $\hat{x}_2^c$ are the filtered-command of $\hat{x}_1$ and $\hat{x}_2$, respectively. From (19) and (20), it can be seen that

$$\begin{aligned}\dot{e}_1 &= \hat{x}_2 + \eta_1 - \dot{x}_1^c, \\ \dot{e}_2 &= bu + \eta_2 - \dot{\hat{x}}_2^c.\end{aligned} \tag{21}$$

Consider the candidate Lyapunov function

$$V_1 = \frac{1}{2}e_1^2. \tag{22}$$

The time derivative of V_1 with respect to time is given by

$$\dot{V}_1 = e_1\left(\hat{x}_2 + \eta_1 - \dot{x}_1^c\right). \tag{23}$$

The virtual controller (i.e., outer-loop controller) can be designed as

$$\hat{x}_2^d = \dot{x}_1^c - \eta_1 - c_1 e_1, \tag{24}$$

where c_1 is a positive definite constant to be designed. Substituting (24) into (23), we have $\dot{V}_1 \le 0$. Pass $\hat{x}_2^d$ through a filter [24], which is shown in Figure 3.

And the state-space model of constrained command filter can be described as

$$\begin{Bmatrix}\dot{q}_1 \\ \dot{q}_2\end{Bmatrix} = \begin{bmatrix}q_2 \\ 2\zeta\omega_n\left[S_R\left(\dfrac{\omega_n^2}{2\xi\omega_n}\left(S_M(v) - q_1\right)\right) - q_2\right]\end{bmatrix}, \tag{25}$$

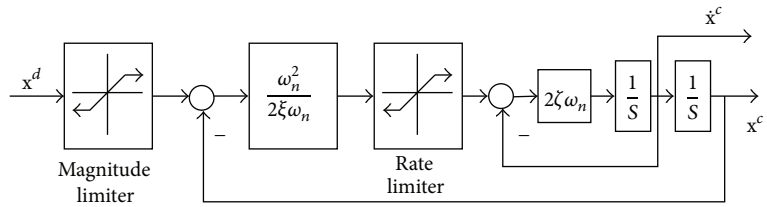

Figure 3: Structure of constrained command filters.

where

$$\begin{bmatrix} q_1 \\ q_2 \end{bmatrix} = \begin{bmatrix} x^c \\ \dot{x}^c \end{bmatrix}, \qquad \upsilon = x^d, \tag{26}$$

and x^c is the output of the constrained command filter.

Therein, ξ and ω_n represent the damping and the bandwidth of filter, respectively.

Redefine tracking error $\bar{e}_1 = e_1 - \epsilon$, and the filter error compensation is designed as

$$\dot{\epsilon} = -c_1\epsilon + \hat{x}_2^c - \hat{x}_2^d. \tag{27}$$

We choose the Lyapunov function

$$V_2 = \frac{1}{2}\bar{e}_1^2 + \frac{1}{2}e_2^2. \tag{28}$$

Then, taking the time derivative of V_2 yields

$$\begin{aligned} \dot{V}_2 &= \bar{e}_1\dot{\bar{e}}_1 + e_2\dot{e}_2 \\ &= \bar{e}_1\left(\hat{x}_2 + \eta_1 - \dot{x}_1^c + c_1\epsilon - \hat{x}_2^c + \hat{x}_2^d\right) \\ &\quad + e_2\left(bu + \eta_2 - \dot{\hat{x}}_2^c\right) \\ &= -\bar{e}_1\left(c_1\bar{e}_1 + \hat{x}_2 - \hat{x}_2^c\right) + e_2\left(bu + \eta_2 - \dot{\hat{x}}_2^c\right) \\ &= -c_1\bar{e}_1^2 - \bar{e}_1e_2 + e_2\left(bu + \eta_2 - \dot{\hat{x}}_2^c\right). \end{aligned} \tag{29}$$

If the global control law is extracted as

$$u = b^{-1}\left(-c_2e_2 - \eta_2 + \bar{e}_1 + \dot{\hat{x}}_2^c\right) \tag{30}$$

the time derivative of Lyapunov function V_2 is described as

$$\dot{V}_2 = -c_1\bar{e}_1^2 - c_2e_2^2 \le 0, \tag{31}$$

where c_2 is also a positive definite constant. Equation (31) means that $\bar{e}_1$ and e_2 are uniformly ultimately bounded. Further, combined with the results of Section 3, we know all error signals are bounded.

5. Simulation Results

Simulations are performed in the MATLAB/SIMULINK environment. From the numerical analysis of the marine power system's chaotic motion, the results can be obtained that when the amplitude $\mu = 1.3$, the chaos will appear in the marine power system under $\lambda = 0.4$, $\rho = 0.2$ and disturbance frequency $\gamma = 0.8$. It can be obtained that the motion state of the marine power system is in Figures 4-5. From Figure 4, it can be seen that the system power angle and the angular velocity of the phase diagram of movement are ergodic, which shows that the system appears in chaos.

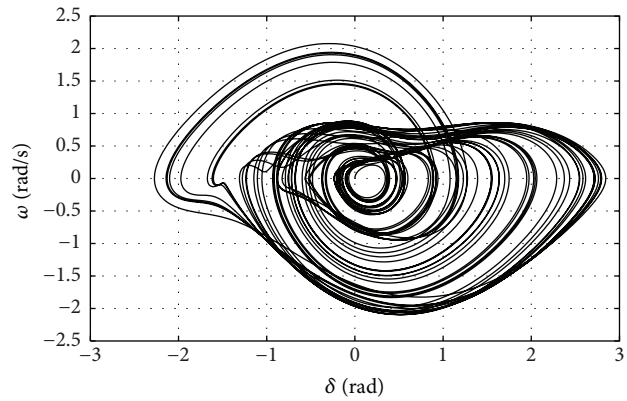

Figure 4: Chaotic attractor under $\mu = 1.3$.

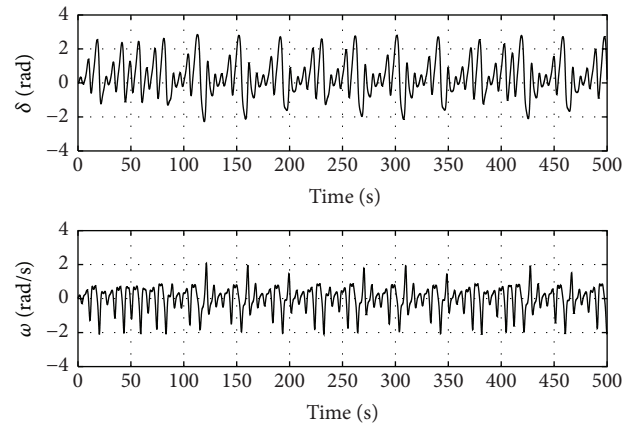

Figure 5: Timing diagram of power angle δ and relative power angle velocity ω.

5.1. Simulation 1 (ESO-Based Model Free Adaptive Command-Filtered Backstepping Control). The parameters of the backstepping controller are chosen as $c_1 = c_2 = 2$. The parameters

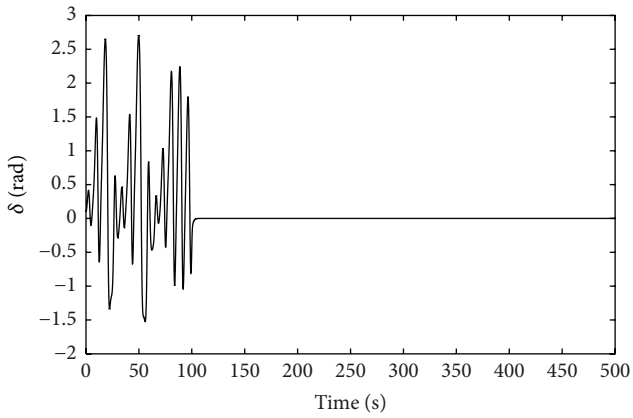

Figure 6: The curve of power angle δ (Simulation 1).

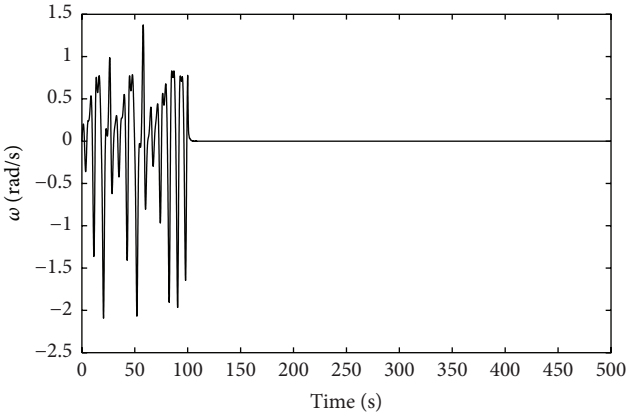

Figure 7: The curve of power angle velocity ω (Simulation 1).

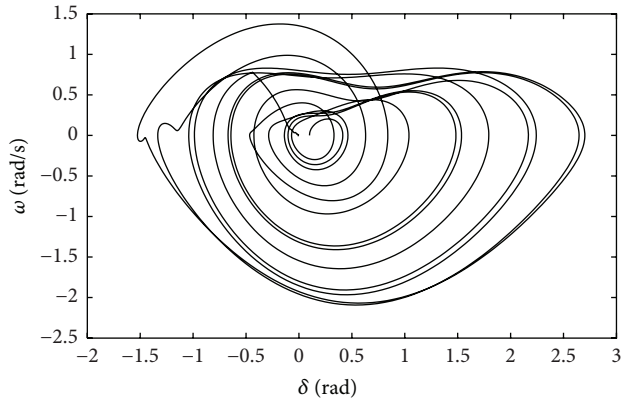

Figure 8: Phase diagram of power angle δ and relative power angle velocity ω (Simulation 1).

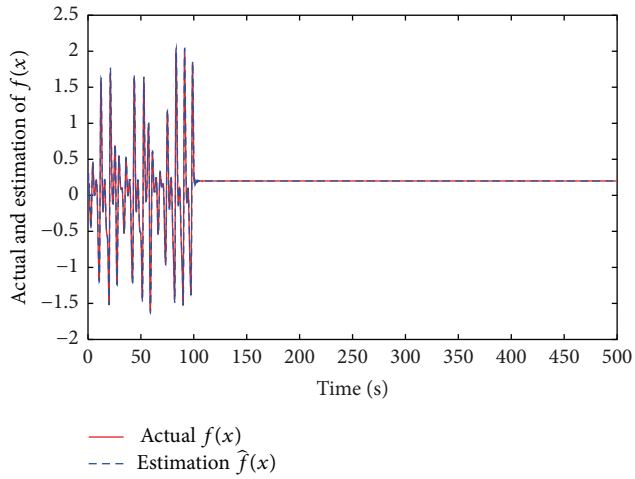

Figure 9: Actual $f(x)$ function and its estimation $\widehat{f}(x)$ (Simulation 1).

of commandfilter are chosen as $\xi = \zeta = 0.1$ and $\omega_n = 20$. The parameters of ESO are designed as $\alpha_1 = \alpha_2 = 0.9$, $\sigma_1 = 100$, $\sigma_2 = 1000$, $l_1 = 10$, $l_2 = 100$, and $l_3 = 1000$. The initial state is $x_0 = [0.1, 0]$. In the following simulation, the control signal u is added to the marine power system when the chaotic motion occurs after 100 seconds. Figures 6 and 7 show the curves of power angle and the angular velocity of marine power system with ESO method. And the phase diagram is expressed in Figure 8. Figure 9 shows the Actual $f(x)$ function and its estimation $\widehat{f}(x)$.

It can be seen from Figures 6 and 7, before 100 seconds, that the power angle and the relative power angle velocity ω are in chaotic state. While the designed controller is added after 100 seconds, the system is quickly stabilized, which indicates that the proposed ESO-based control algorithm has a very reliable and stable ability for the marine power system's chaotic motion.

5.2. Simulation 2 (NNO-Based Model Free Adaptive Command-Filtered Backstepping Control). In Simulation 2, the same parameters of the backstepping controller and command-filter are chosen as Simulation 1. The number of nodes of neural network basis function is chosen as 10. The parameters of NNO are designed as $K = [1000, 2000]^T$, $b_0 = [0, 1]^T$, $\Upsilon = \text{diag}[5 \times 10^4]$, and $\kappa = 0.001$. The initial states of the marine power system and NNO are $x_0 = \widehat{x}_0 = [0.1, 0]$. In the following simulation, the control signal u is also added to the marine power system when the chaotic motion occurs after 100 seconds. Figures 10 and 11 show the curves of power angle and the angular velocity of marine power system under NNO method. And the phase diagram is shown in Figure 12. Figure 13 shows the actual $f(x)$ function and the estimation $\widehat{f}(x)$.

It can be seen from Figures 10 and 11, after 100 seconds, that the designed controller is added to the chaotic marine power system, and the system is quickly stabilized, which indicates that the proposed NNO-based control algorithm also has a very reliable and stable ability for the marine power system's chaotic motion.

6. Conclusion

Based on observer techniques, two novel model free adaptive command-filtered backstepping control methods are proposed for marine power systems. In the developed two model

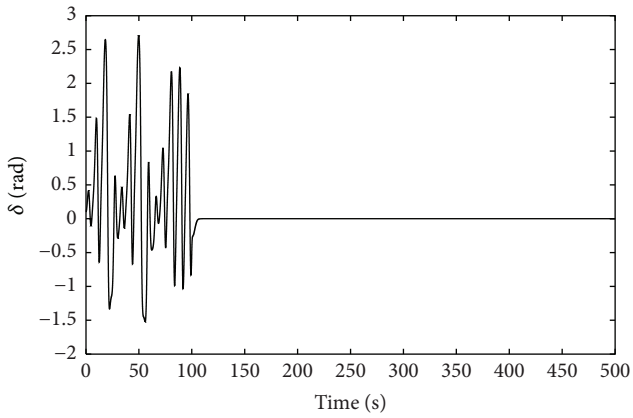

FIGURE 10: The curve of power angle δ (Simulation 2).

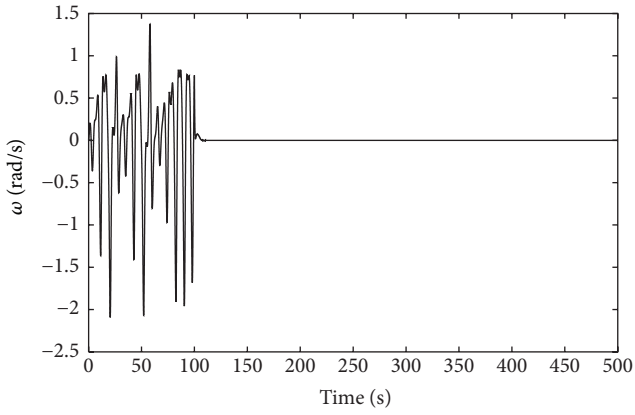

FIGURE 11: The curve of power angle velocity ω (Simulation 2).

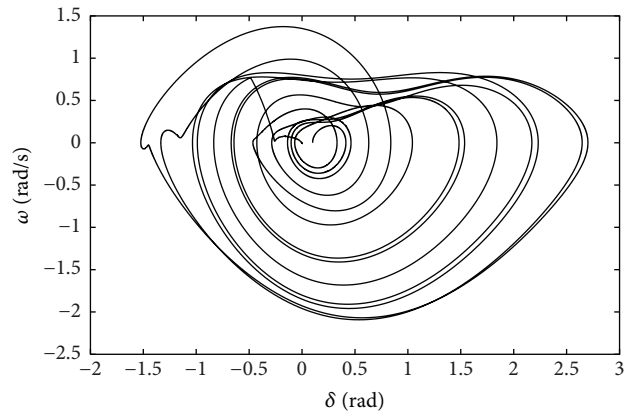

FIGURE 12: Phase diagram of power angle δ and relative power angle velocity ω (Simulation 2).

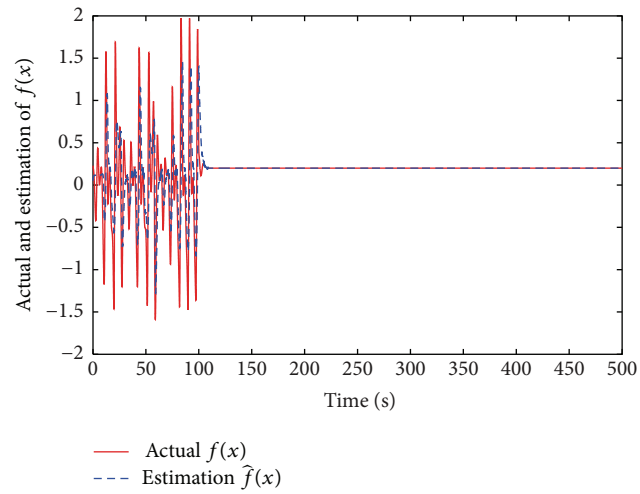

FIGURE 13: Actual $f(x)$ function and its estimation $\hat{f}(x)$ (Simulation 2).

free adaptive command-filtered backstepping controls, there are three main problems solved. They are the following: (1) Velocity signal does not need to be known. The proposed control algorithms can achieve the closed-loop stability without speed sensor. (2) The proposed control methods do not need dynamic mathematical model of marine power systems. (3) The proposed two controls can eliminate the impact of derivative signal and control saturation. In addition, the stability analysis is given for closed-loop control system. Simulation results show that the proposed method not only guarantees the closed-loop stability of the controlled marine power system, but also well identifies the velocity state and the unknown dynamic model.

Conflict of Interests

The authors declare that there is no conflict of interests regarding the publication of this paper.

Acknowledgments

This work was partially supported by the National Natural Science Foundation of China (61490703, 61473250, and 61403161), the Fundamental Research Funds for the Central Universities (JUSRP11562), and the Natural Science Foundation of Jiangsu Higher Education Institution (14KJB120013).

References

[1] S. E. Ben Elghali, M. E. H. Benbouzid, and J.-F. Charpentier, "Modelling and control of a marine current turbine-driven doubly fed induction generator," *IET Renewable Power Generation*, vol. 4, no. 1, pp. 1–11, 2010.

[2] H.-K. Chen, T.-N. Lin, and J.-H. Chen, "Dynamic analysis, controlling chaos and chaotification of a SMIB power system," *Chaos, Solitons and Fractals*, vol. 24, no. 5, pp. 1307–1315, 2005.

[3] X. Li and C. A. Cañizares, "Chaotic behavior observations in a power system model," in *Proceedings of the IEEE Bucharest PowerTech: Innovative Ideas Toward the Electrical Grid of the Future*, Bucharest, Romania, July 2009.

[4] G. Chen, "Control and anti-control of chaos," *IEEE Circuits and Systems Society Newsletter*, vol. 9, no. 1, pp. 181–186, 1998.

[5] S. Boccaletti, C. Grebogi, Y.-C. Lai, H. Mancini, and D. Maza, "The control of chaos: theory and applications," *Physics Reports*, vol. 329, no. 3, pp. 103–197, 2000.

[6] C.-C. Hwang, J.-Y. Hsieh, and R.-S. Lin, "A linear continuous feedback control of Chua's circuit," *Chaos, Solitons & Fractals*, vol. 8, no. 9, pp. 1507–1515, 1997.

[7] M. Feki, "An adaptive feedback control of linearizable chaotic systems," *Chaos, Solitons & Fractals*, vol. 15, no. 5, pp. 883–890, 2003.

[8] Z.-S. Hou and Z. Wang, "From model-based control to data-driven control: survey, classification and perspective," *Information Sciences*, vol. 235, pp. 3–35, 2013.

[9] J. A. Farrell, M. Polycarpou, and M. Sharma, "Longitudinal flight path control using on-line function approximation," *Journal of Guidance, Control, and Dynamics*, vol. 26, no. 6, pp. 885–897, 2003.

[10] X.-G. Yan, S. K. Spurgeon, and C. Edwards, "State and parameter estimation for nonlinear delay systems using sliding mode techniques," *IEEE Transactions on Automatic Control*, vol. 58, no. 4, pp. 1023–1029, 2013.

[11] X.-G. Yan, S. K. Spurgeon, and C. Edwards, "Memoryless static output feedback sliding mode control for nonlinear systems with delayed disturbances," *Institute of Electrical and Electronics Engineers. Transactions on Automatic Control*, vol. 59, no. 7, pp. 1906–1912, 2014.

[12] D. Swaroop, J. K. Hedrick, P. P. Yip, and J. C. Gerdes, "Dynamic surface control for a class of nonlinear systems," *IEEE Transactions on Automatic Control*, vol. 45, no. 10, pp. 1893–1899, 2000.

[13] M. Zhang, L. Yin, and L. Qiao, "Adaptive fault tolerant attitude control for cube satellite in low earth orbit based on dynamic neural network," *International Journal of Innovative Computing, Information and Control*, vol. 10, no. 5, pp. 1843–1852, 2014.

[14] N. Chen, F. Song, G. Li, X. Sun, and C. Ai, "An adaptive sliding mode backstepping control for the mobile manipulator with nonholonomic constraints," *Communications in Nonlinear Science and Numerical Simulation*, vol. 18, no. 10, pp. 2885–2899, 2013.

[15] Y. Xia, P. Shi, G. P. Liu, D. Rees, and J. Han, "Active disturbance rejection control for uncertain multivariable systems with time-delay," *IET Control Theory & Applications*, vol. 1, no. 1, pp. 75–81, 2007.

[16] D. Xu, B. Jiang, and P. Shi, "A novel model-free adaptive control design for multivariable industrial processes," *IEEE Transactions on Industrial Electronics*, vol. 61, no. 11, pp. 6391–6398, 2014.

[17] D. Xu, B. Jiang, and P. Shi, "Adaptive observer based data-driven control for nonlinear discrete-time processes," *IEEE Transactions on Automation Science and Engineering*, vol. 11, no. 4, pp. 1037–1045, 2014.

[18] Z. Hou and S. Jin, "A novel data-driven control approach for a class of discrete-time nonlinear systems," *IEEE Transactions on Control Systems Technology*, vol. 19, no. 6, pp. 1549–1558, 2011.

[19] X. Su, P. Shi, L. Wu, and M. V. Basin, "Reliable filtering with strict dissipativity for T-S fuzzy time-delay systems," *IEEE Transactions on Cybernetics*, vol. 44, no. 12, pp. 2470–2483, 2014.

[20] J. Han, "From PID to active disturbance rejection control," *IEEE Transactions on Industrial Electronics*, vol. 56, no. 3, pp. 900–906, 2009.

[21] Q. Zhou, P. Shi, S. Xu, and H. Li, "Observer-based adaptive neural network control for nonlinear stochastic systems with time delay," *IEEE Transactions on Neural Networks and Learning Systems*, vol. 24, no. 1, pp. 71–80, 2013.

[22] D. Xu, B. Jiang, M. Qian, and J. Zhao, "Terminal sliding mode control using adaptive fuzzy-neural observer," *Mathematical Problems in Engineering*, vol. 2013, Article ID 958958, 8 pages, 2013.

[23] J. A. Farrell, M. Polycarpou, M. Sharma, and W. Dong, "Command filtered backstepping," *IEEE Transactions on Automatic Control*, vol. 54, no. 6, pp. 1391–1395, 2009.

[24] B. Jiang, D. Xu, P. Shi, and C. C. Lim, "Adaptive neural observer-based backstepping fault tolerant control for near space vehicle under control effector damage," *IET Control Theory and Applications*, vol. 8, no. 9, pp. 658–666, 2014.